JAAS

ROYAL SOCIETY OF CHEMISTRY

PAPER

View Article Online
View Journal

Cite this: DOI: 10.1039/d6ja00052e

Sensitive determination of biologically important transition metals by ICP-QMS using micro-ultrasonic single droplet nebulization

Yang Yu,[a] Junhang Dong,[ae] Baoliang Zhong,*[c] Xiaoqing Jin,[d] Zhujun Dai,[a] Linjie Chen,[a] Yu Li,[b] Jing Chen,*[c] Huan Tian,[b] Hongtao Zheng,[b] Xing Liu[a] and Zhenli Zhu *[ab]

The determination of trace transition metals in biological samples is often limited by extremely small sample volumes and complex matrix effects. In this work, a highly sensitive analytical method for the simultaneous determination of Mn, Co, Ni, Cu, and Zn in micro-volume samples was developed by coupling micro-ultrasonic single-droplet nebulization (MUSDN) with inductively coupled plasma quadrupole mass spectrometry (ICP-QMS). Key parameters were systematically optimized, with a particular focus on the evaluation of a Pt nebulizer sheet to reduce background equivalent concentrations (BECs). In addition, Ge was selected as the internal standard to effectively compensate for instrumental drift and matrix effects, thereby improving analytical stability. Under optimized conditions, the method exhibited excellent linearity ($R^2 \geq 0.999$) and precision (RSDs ~2%), while the achieved sensitivity enhancement (11.5–19.6-fold) was consistent with the previously reported advantages of MUSDN. The method exhibited good tolerance toward high-salt and organic matrices, thus enabling accurate analysis of diluted serum samples without digestion. Its feasibility and reliability were further validated through the analysis of certified serum reference materials and real samples. These results demonstrate that MUSDN-ICP-QMS is a robust and efficient approach for trace metal analysis in volume-limited biological samples.

Received 9th February 2026
Accepted 17th April 2026

DOI: 10.1039/d6ja00052e

rsc.li/jaas

Introduction

Transition metal elements such as Mn, Co, Ni, Cu, and Zn play critical roles in a wide range of biological processes, serving as essential cofactors in enzymatic pathways related to energy metabolism, DNA replication, signal transduction and other vital functions.[1–8] Consequently, the accurate determination of these trace metals in biological specimens is of great importance for advancing biomedical, environmental, and toxicological research.[9–13] Despite their importance, quantitative analysis of metal elements in micro-volume serum samples remains challenging. This difficulty arises from the combination of inherently low endogenous concentrations and the extremely limited sample volumes typically available.[14,15]

ICP-QMS is a leading technique for trace element analysis. Nevertheless, its conventional pneumatic nebulization (PN) sample introduction system suffers from its inherently low efficiency (typically <5%) making it unsuitable for highly sensitive analysis of micro-volume samples. To overcome this limitation, several high-efficiency sample introduction approaches have been developed, including electrothermal vaporization (ETV),[16] hydride generation (HG),[17] membrane desolvation (MD),[18–20] and direct injection nebulization (DIN).[21,22] These techniques can markedly enhance analytical sensitivity. However, each presents intrinsic drawbacks when applied to simultaneous multi-element analysis of biological matrices: ETV typically offers low throughput,[16,23] HG is restricted to hydride-forming elements,[17] MD suffers from pronounced memory effects[19,20] and DIN is prone to clogging.[24–26]

Recently, micro-ultrasonic nebulization (MUN) has attracted increasing attention because of its high efficiency, low cost, and minimal sample consumption.[27–29] Recently, our group developed a high efficiency MUN sample introduction unit for elemental analysis by ICP-MS, achieving near-complete sample introduction and exceptional analytical sensitivity.[30] In subsequent work, we further adapted this approach for high precision isotope analysis through multi-collector inductively coupled plasma mass spectrometry (MC-ICPMS) by implementing an

[a]State Key Laboratory of Geomicrobiology and Environmental Changes, China University of Geosciences, Wuhan, Hubei 430074, China
[b]Faculty of Materials Science and Chemistry, China University of Geosciences, Wuhan, Hubei 430074, China
[c]Clinical Psychology Department, Wuhan Mental Health Center, Wuhan, Hubei Province, China
[d]Emergency Center, Zhongnan Hospital of Wuhan University, No. 169 Donghu Road, Wuhan, 430071, Hubei, China
[e]Research Institute of Petroleum Engineering, Shengli Oilfield Company, SINOPEC, Dongying 257000, China

updated single droplet MUN system (MUSDN), which greatly reduced the required sample volume.[31] However, despite these advancements, the applicability of MUSDN for routine multi-element quantification in volume-limited samples has not yet been systematically investigated.

In this study, we comprehensively evaluated the feasibility of MUSDN for the determination of five biologically essential transition metals (Mn, Co, Ni, Cu, Zn) by ICP-QMS. Several key operational parameters, including MUN sheet material, droplet volume, and internal standard, were optimized. The method's detection limits, matrix tolerance, and analytical accuracy were also systematically assessed. Finally, its practical applicability was demonstrated through the analysis of certified serum reference materials and real samples.

Experimental section

Reagents and chemicals

High-purity reagents were used throughout this work unless otherwise specified. Ultrapure water (>18.2 MΩ cm) was produced using a Milli-Q water purification system (Millipore gradient, Merck Millipore, Darmstadt, Germany). High-purity nitric acid was obtained through double sub-boiling distillation. Analytical-grade *n*-butanol was supplied by Tianjin Fuyu Fine Chemical Co., Ltd, and Triton™ X-100 (analytical grade) was purchased from Macklin. A series of standard working solutions with varying concentrations were prepared by diluting single-element stock solutions (Sc, Mn, Co, Ni, Cu, Zn, Ge, Rh, In; 1000 μg mL^{-1}; NCS, Beijing, P.R. China). Two serum CRMs, Seronorm™ trace-element Serum L-1 and L-2 RUO, were used and stored in darkness at 2–8 °C prior to analysis.

Clinical subjects and sample harvesting

This study was conducted in accordance with the principles of the Declaration of Helsinki, and the study protocol was approved by the ethical committees of China University of Geosciences (Wuhan, China) and Wuhan Zhongnan Hospital of Wuhan University. All serum samples from patients were collected from Wuhan Zhongnan Hospital of Wuhan University, and signed informed consents were obtained from participants or their authorized representatives prior to all study procedures.

Sample preparation

To evaluate matrix effects, a series of synthetic matrix samples were prepared. Specifically, individual matrix solutions containing Na, K, Ca, and Mg were generated. The procedure involved evaporating aliquots of single-element standard stock solutions to dryness and reconstituting the residues with appropriate mixed analyte standard solutions. This process yielded primary matrix solutions with a target concentration of 10 000 mg L^{-1} for each respective matrix element. These solutions were subsequently serially diluted to produce the final working calibration standards used for the matrix effect study.

Serum samples were digested in closed PTFE-lined bombs for trace element analysis. Approximately 200 μL of serum was accurately weighed, mixed with 1 mL of concentrated HNO_3, and heated at 190 °C for 24 h. After cooling, the digest was transferred to a PFA beaker and evaporated to near-dryness at 105 °C. Residual acid was removed by adding 0.2 mL of deionized water and evaporating to dryness. The final residue was dissolved in an acid solution containing 10 μg L^{-1} Ge (internal standard) prior to analysis. The samples without digestion (direct dilution method) were prepared as follows: 5 μL of the sample was transferred into a 100 μL vial using a micropipette. Then, 5 μL of a 20 μg L^{-1} Ge internal standard solution (in dilute HNO_3) was added, and the mixture was mixed thoroughly. Subsequently, 4 μL of the mixed solution was taken and introduced for analysis.

To prevent sample-to-sample carryover, three consecutive washes with 4 μL of 2% HNO_3 were performed after each sample measurement. This procedure effectively reduced residual signals to blank levels for all five elements.

Instrumentation

The MUSDN sample introduction system was designed and developed by Dong *et al.* from our research group.[31] The system comprises a commercially available MUN sheet, which converts microliter liquid droplets into fine aerosol, and a no-waste spray chamber for ordered aerosol transport.[30] The MUN sheet is mounted onto the spray chamber *via* a connecting ring with an integrated O-ring seal, as described previously.[31] A schematic diagram of the MUSDN-ICP-QMS configuration is shown in Fig. 1 stainless steel and platinum MUN sheets (Suzhou Chirong Precision Electronics Co., Ltd) were used in this study; both types contain laser-drilled micro-orifices with a batch-to-batch diameter variation below 5%. The key orifice specifications include an inlet diameter of 30 μm, an outlet diameter of 2.5 μm, and a drilling diameter of 0.5 mm, corresponding to 21 orifices per sheet.[31]

The MUSDN system was driven by a function generator (DG 1022 Z, Rigol Technologies, Inc.), delivering a 50% duty cycle square wave. The driving voltage was fixed at 16 V to ensure efficient droplet nebulization, while the operating frequencies were optimized at 110 kHz for the stainless-steel sheet and 103 kHz for the platinum sheet. Sample droplets were precisely loaded onto the center of the MUN sheet using an Eppendorf Research® plus manual pipette (0.5–10 μL range).

Elemental quantification was performed using an Agilent 7900 ICP-QMS at the Faculty of Materials Science and Chemistry, China University of Geosciences (Wuhan). A pneumatic nebulizer equipped with a quartz spray chamber was employed for conventional sample introduction to optimize the ICP-QMS operating parameters and to obtain reference quantitative values for real samples, thereby validating the accuracy of the proposed MUSDN based method. The detailed instrumental parameters are summarized in Table 1.

Results and discussion

Feasibility of MUSDN for high sensitivity elemental analysis by ICP-QMS

To evaluate the feasibility of MUSDN-ICP-QMS for highly sensitive analysis of biologically essential transition metals, we

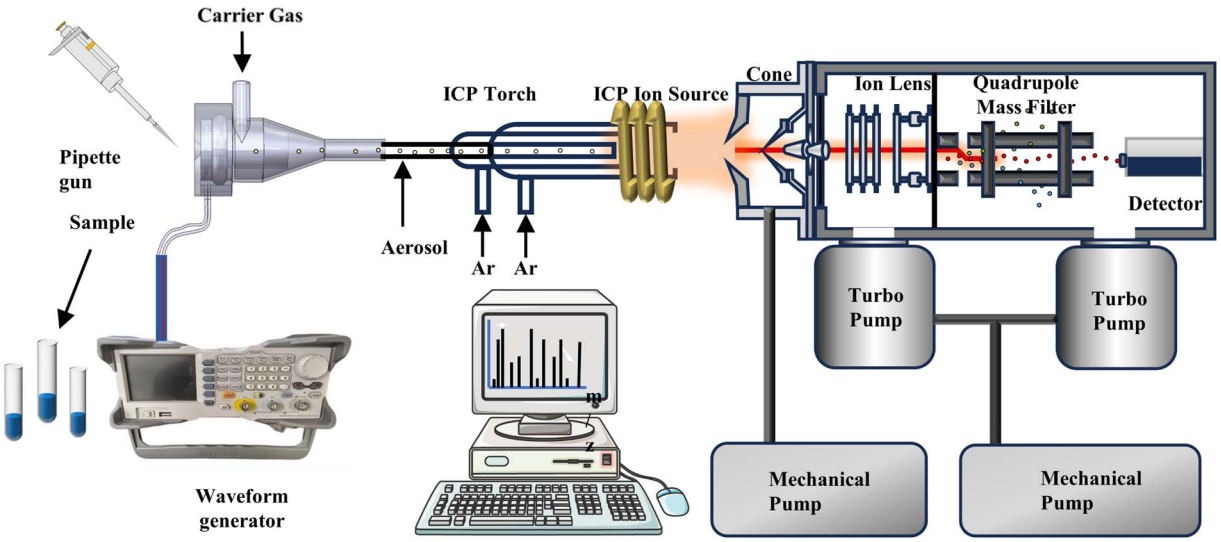

Fig. 1 Schematic diagram of MUSDN-ICP-QMS experimental setup.

Table 1 Operating conditions for the PN-ICP-QMS and MUSDN-ICP-QMS

Parameters	PN-ICP-QMS	MUSDN-ICP-QMS
RF power (W)	1550	1550
RF matching (V)	1.8	1.5
Sampling depth (mm)	8.0	8.0
Nebulizer gas flow (L min^{-1})	1.05	1.30
Plasma gas flow (L min^{-1})	15	15
Auxiliary gas flow (L min^{-1})	0.90	0.90
Extraction voltage 1 (V)	−10.2	−10.2
Extraction voltage 2 (V)	−235.0	−235.0
Bias voltage (V)	−120	−120
Lens voltage (V)	8.5	8.5
Skimmer cone	AT7902X-Ni	AT7902X-Ni
Sampling cone	AT7701-Ni	AT7701-Ni
Acquisition mode	Peak hopping	Time resolved analysis (TRA)
Mass of elements	*e.g.*, ^{55}Mn, ^{59}Co, ^{60}Ni, ^{65}Cu, ^{66}Zn, ^{72}Ge	*e.g.*, ^{55}Mn, ^{59}Co, ^{60}Ni, ^{65}Cu, ^{66}Zn, ^{72}Ge
Integ time/mass (s)	0.1	0.1

first examined the signal peak profiles and reproducibility, followed by an assessment of analytical sensitivity relative to PN-ICP-QMS. In this experiment, the stainless-steel MUN nebulizer previously described by Dong *et al.*[31] was employed. Conventional PN-ICP-QMS and MUSDN-ICP-QMS measurements were performed sequentially on the same day using a mixed standard solution containing Mn, Co, Ni, Cu, and Zn at a concentration of 10 μg L^{-1}. As shown in Fig. 2, a single 2 μL droplet generated a transient signal with a duration of approximately 4.2 seconds with MUSDN-ICP-QMS, consistent with previous work.[31] Successive injections produced nearly identical peak shapes, indicating excellent operational consistency. The relative standard deviations (RSDs) of 11 consecutive measurements ranged from 5.2% (Ni) to 6.8% (Mn), demonstrating that the MUSDN system provides acceptable stability suitable for quantitative analysis. Furthermore, to verify the robustness of the plasma conditions under the low sample consumption of MUSDN, the oxide and doubly charged ion ratios were assessed

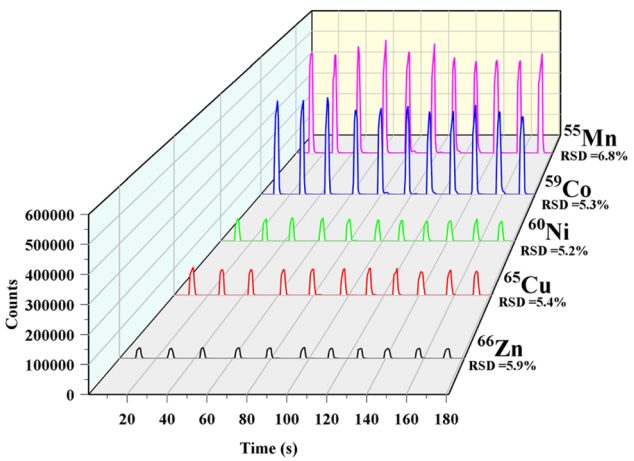

Fig. 2 Signal profiles from 11 replicate MUSDN-ICP-QMS injections. The RSDs of the peak areas for each element were determined.

by performing 11 consecutive injections of a 10 μg L^{-1} Ce standard solution. The average CeO^+/Ce^+ and Ce^{2+}/Ce^+ ratios were 3.3% and 5.6%, respectively. These low and stable values indicate that the MUSDN sampling method does not compromise plasma robustness, effectively minimizing spectral interferences from oxide and doubly charged species during subsequent trace element analysis in complex biological samples.

Previous work in our group has demonstrated that this sample introduction system can enhance sensitivity by more than an order of magnitude.[30] In summary, MUSDN-ICP-QMS offers good reproducibility and sensitivity for the analysis of transition metals in precious and volume-limited samples. However, there remains potential for further enhancement of its analytical performance. Factors such as the nebulizer sheet material may influence the BEC and signal-to-noise ratio (S/N), while optimizing the droplet volume and selecting an appropriate internal standard could improve the reproducibility and accuracy. Therefore, subsequent optimization efforts will focus on systematically improving these aspects to further enhance the analytical capability of the MUSDN-ICP-QMS system.

Material optimization of the MUN sheet

Stainless steel contains Fe, Ni, Cr, Mo, and Ti, and various minor elements (*e.g.* Mn, Cu, Zn, Co, and Si), any of which may contribute to background contamination during single-droplet aerosol generation. Although aerosol formation in MUSDN is transient, dissolution or trace release from the nebulizer sheet could still elevate elemental background. Therefore, we first evaluated whether replacing the stainless-steel MUN with a Pt MUN sheet could reduce BECs and improve S/N. The S/N were calculated based on 11 consecutive measurements of a 10 μg L^{-1} multi-element standard solution.

Table 2 summarizes the S/N and BECs results obtained using the two materials. Overall, the Pt sheet provided higher S/N values for Co, Ni, Cu, and Zn. When a 10 μg L^{-1} multi-element standard solution was measured 11 times, the Pt sheet yielded S/N values of 2123.0 (Co), 5353.9 (Ni), 2687.8 (Cu), and 2471.6 (Zn), all substantially higher than those obtained with the stainless steel sheet, which were 1894.8 (Co), 183.3 (Ni), 1258.2 (Cu), and 1513.5 (Zn), respectively. Mn was the only exception for which the Pt sheet produced a slightly lower S/N (162.7) compared with the stainless steel (256.5).

Table 2 Comparison of S/N and BECs for MUSDN (stainless steel)-ICP-QMS *versus* MUSDN(Pt)-ICP-QMS

	MUSDN (stainless steel)-ICP-QMS		MUSDN(Pt)-ICP-QMS	
Element	S/N	BEC (μg L^{-1})	S/N	BEC (μg L^{-1})
^{55}Mn	256.5	1.41	162.7	1.93
^{59}Co	1894.8	0.14	2123.0	0.13
^{60}Ni	183.3	0.68	5353.9	0.04
^{65}Cu	1258.2	0.15	2687.8	0.08
^{66}Zn	1513.5	0.12	2471.6	0.10

The similar trend was reflected in BEC values. Pt sheet resulted in lower BECs for Co (0.13 μg L^{-1}), Ni (0.04 μg L^{-1}), Cu (0.08 μg L^{-1}), and Zn (0.10 μg L^{-1}), compared with stainless steel sheet (0.14, 0.68, 0.15, and 0.12 μg L^{-1}, respectively). The most pronounced improvement was observed for Ni (a 17-fold reduction), which is consistent with the high nickel content of stainless steel being a major source of background contamination. For Co and Zn, where the stainless steel background was already relatively low, the improvements were more modest. Again, Mn was the exception, with a slightly higher BEC value for the Pt sheet (1.93 μg L^{-1}) relative to stainless steel (1.41 μg L^{-1}). These results demonstrate that, with the exception of Mn, the Pt sheet significantly reduces BEC and improves S/N for the other four elements. The inferior performance for Mn with the Pt sheet might be due to a higher background level of Mn in the platinum material itself, or possibly due to contamination during the fabrication process. The notably improved performance for Ni is consistent with the high nickel content of stainless-steel, which likely contributes to elevated Ni background. In conclusion, replacing the stainless steel with a Pt sheet effectively reduces background dissolution in the MUSDN-ICP-QMS system, thereby lowering BEC for most elements.

Droplet volume optimization for MUSDN sampling

Pipetting inaccuracy and residual liquid on the nebulizer are potential sources of imprecision in MUSDN-ICP-QMS. Increasing the dispensed droplet volume is expected to mitigate these effects. To examine the influence of sample droplet volume on analytical precision, a mixed standard solution containing Mn, Co, Ni, Cu, and Zn (10 μg L^{-1} each) was analyzed using volumes of 1, 2, 3, 4, and 5 μL, with 33 consecutive measurements per volume. As shown in Fig. 3, RSDs for all five elements decreased progressively as the droplet volume increased, with substantial improvement from 1 to 4 μL. Beyond 4 μL, the RSDs reached a plateau, indicating further increases in volume no longer significantly enhance reproducibility. The

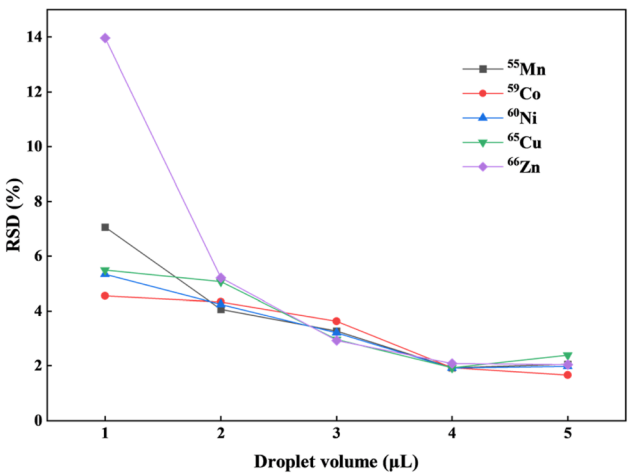

Fig. 3 Relationship between RSD and sample droplet volume in MUSDN-ICP-QMS.

improvement at smaller volumes can be attributed to reduced relative pipetting error and diminished influence of residual liquid on the nebulizer surface. Once the volume reached approximately 4 μL, both pipetting and nebulization became highly stable, establishing 4 μL as the optimal volume for MUSDN sampling. Under these optimized conditions, the MUSDN sampling method achieved RSDs of approximately 2%, demonstrating its excellent reproducibility even when operating with low sample volumes.

Evaluation of matrix interference tolerance

Internal standardization was evaluated as a strategy to further improve analytical stability and precision in MUSDN-ICP-QMS. Among the four internal standards tested (Sc, Ge, Rh, and In), all reduced signal variability; however, Ge provided the most effective correction across all analytes, yielding the lowest RSDs. This can be attributed to the close match in ionization energy (7.90 eV) and mass (m/z 72) between Ge and the target analytes (Mn, Co, Ni, Cu, Zn), which enables effective compensation for matrix effects and instrumental drift. In contrast, the other tested internal standards—Sc (IE = 6.56 eV), Rh (IE = 7.46 eV), and In (IE = 5.79 eV), resulted in either overcorrection (Sc) or less stable correction (Rh, In) under the applied plasma conditions, likely due to differences in ionization efficiency or mass-to-charge characteristics. Consequently, Ge was selected as the optimal internal standard for this analytical method.

To evaluate matrix effects, mixed standard solutions containing Mn, Co, Ni, Cu, Zn, and Ge were prepared in two representative matrices: a high-dissolved-solid matrix and an organic matrix. These matrices consisted of varying concentrations of $Ca(NO_3)_2$, KNO_3, $Mg(NO_3)_2$, $NaNO_3$, Triton X-100, and n-butanol. Unlike previous studies in which all analytes were spiked with concentration of 10 μg L^{-1}, the spike concentrations were adjusted for the high-dissolved-solid matrix containing $NaNO_3$. This adjustment was necessary because the $NaNO_3$ reagent used exhibited elevated blank signals for Cu and Zn; thus, their concentrations in the $NaNO_3$-containing mixed standard were increased to 100 μg L^{-1} to ensure reliable blank subtraction and the acquisition of meaningful net analytical signals. All measurements were used a 4 μL injection volume, and analyte recoveries were calculated relative to those obtained in a 2% nitric acid matrix.

The influence of the matrix elements on signal duration in the MUSDN-ICP-QMS was firstly investigated by analyzing solutions containing 10 μg L^{-1} Mn/Co/Ni/Ge and 100 μg L^{-1} Cu/Zn in $NaNO_3$ matrices with Na concentrations ranging from 0 to 10 000 mg L^{-1}. As shown in Fig. 4A–F, all elements exhibited highly consistent temporal signal profiles across different $NaNO_3$ concentrations. Each curve followed the characteristic pulse-injection behavior, including a rapid rise, a stable plateau, and a fast decline, with nearly identical peak onset time, plateau duration, and signal offset time. Although signal intensity gradually decreased with increasing $NaNO_3$ concentration due to matrix-induced suppression, no signal interruptions, plateau distortions, or premature signal drops (which are typical indicators of nebulizer clogging) were observed even at the 10 000 mg L^{-1} Na high-salt condition. These results directly demonstrate that the MUSDN system enables stable and unobstructed sample introduction under high-salt conditions, effectively preventing nebulizer clogging and ensuring compatibility with saline samples.

As illustrated in Fig. S1A and detailed in Table S1, the recoveries of all the analytes decreased progressively with increasing dissolved solids content, reflecting typical matrix-induced suppression effects.[32] In contrast, increasing organic content led to enhanced analyte recoveries (Fig. S1B), consistent with carbon-induced signal enhancement for elements with relatively high ionization energies.[33] These opposing trends arise from different mechanisms: high concentration of inorganic salts suppress analyte signals primarily through space charge effects and reduced plasma ionization efficiency, whereas organic substances act as additional carbon source that promotes analyte ionization.[32,33]

Without internal standard correction, most normalized signals fell outside the ±15% recovery acceptance range required for clinical quality control (Fig. S1A and S1B). In contrast, correction using Ge as an internal standard, based on the normalized $^{55}Mn/^{72}Ge$, $^{59}Co/^{72}Ge$, $^{60}Ni/^{72}Ge$, $^{65}Cu/^{72}Ge$ and $^{66}Zn/^{72}Ge$ ratios shown in Fig. S1C and S1D, effectively compensated for both inorganic and organic matrix effects. After internal standard correction, the majority of the recoveries were confined within the 85–115% range, fully meeting clinical quality control requirements.

Overall, these results confirm that MUSDN-ICP-QMS exhibits strong tolerance toward both high-salt and organic matrices. Moreover, the combination of MUSDN sampling with Ge internal standardization provides a robust and reliable strategy for minimizing matrix-induced interferences in the analysis of complex biological samples.

Evaluation of analytical performance for MUSDN-ICP-QMS

Under the optimized experimental conditions (Table 1), employing a platinum MUN nebulizer, a 4 μL sample volume, and ^{72}Ge as the internal standard, external calibration curves were established using standard solutions at concentrations of 0, 1, 5, 10, 20, 50 μg L^{-1}. As shown in Fig. S2A–E, excellent linearity was obtained for all analytes over the investigated concentration range, with correlation coefficients (R^2) between 0.99901 and 1.00000. The analytical performance of the MUSDN-ICP-QMS method, including limits of detection (LOD), absolute limit of detection (ALOD) and sensitivity were systematically evaluated and compared with those obtained using conventional PN-ICP-QMS (Table 3). The LODs for the five target elements ranged from 0.014 μg L^{-1} (Ni) to 0.073 μg L^{-1} (Mn). Although three elements exhibited slightly higher LOD compared to PN-ICP-QMS when analyzed using the MUSDN system. Owing to the markedly enhanced sensitivity (11.5–19.6-fold, Fig. S2F) combined with an ultra-low sample consumption of only 4 μL, the ALODs obtained with MUSDN-ICP-QMS were improved by 1–2 orders of magnitude relative to PN-ICP-QMS. This substantial reduction in ALODs is particularly critical for the analysis of trace transition metals in volume-limited

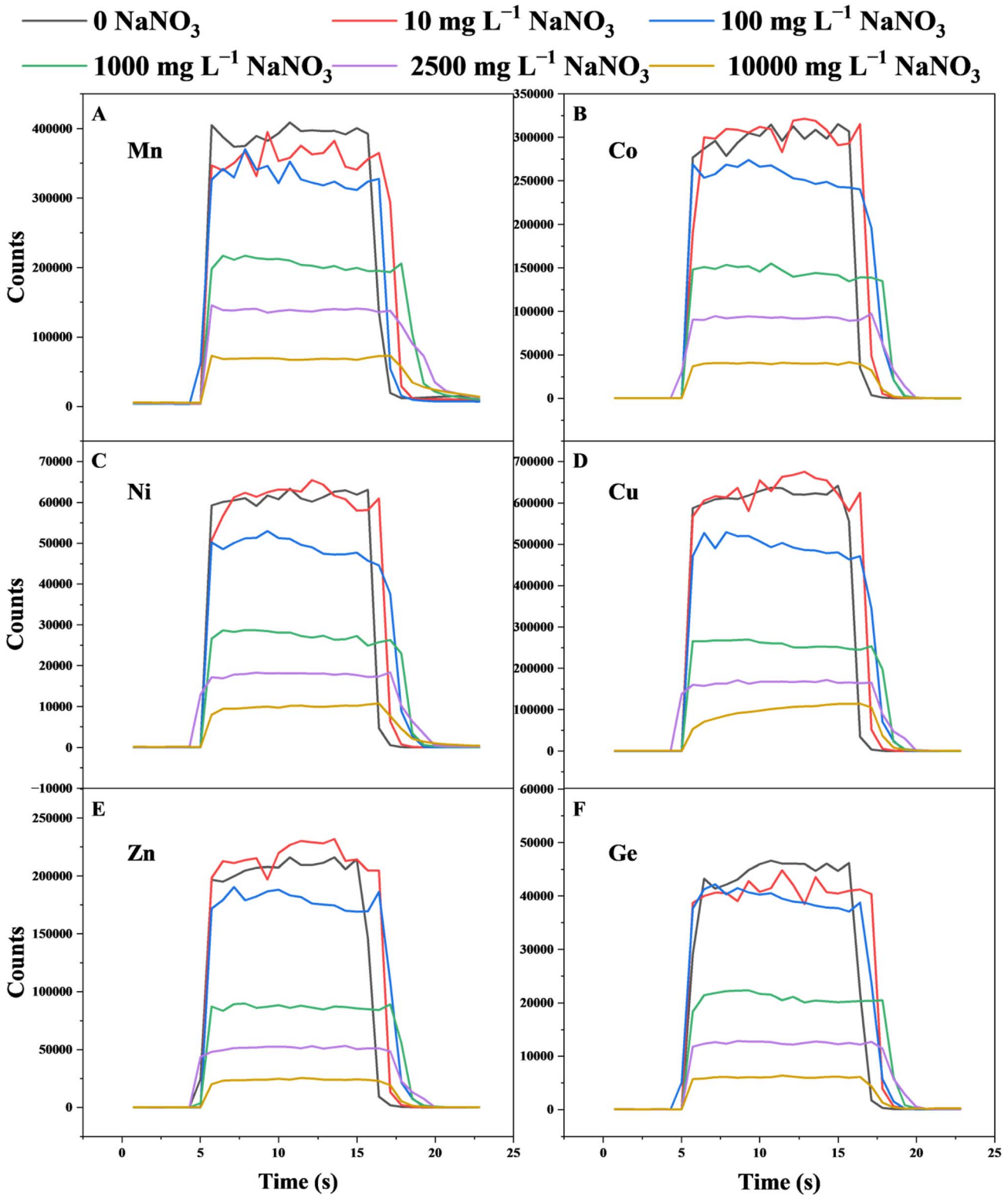

Fig. 4 Signal response curves of Mn (A), Co (B), Ni (C), Cu (D), Zn (E), and Ge (F) *via* MUSDN-ICP-QMS under different $NaNO_3$ matrix conditions.

biological and clinical samples. Overall, these results demonstrate that the MUSDN introduction system exhibits excellent analytical performance and is well-suited for the highly sensitive analysis of trace elements in small-volume samples.

Accuracy validation and application

To validate the accuracy of the proposed method, two certified reference materials (CRMs) of digested serum were analyzed. After a two-fold dilution, only 4 μL of the sample was introduced

Table 3 Comparison of analytical performance between PN-ICP-QMS and MUSDN-ICP-QMS

	MUSDN-ICP-QMS			PN-ICP-QMS		
Element	LOD (μg L^{-1})	ALOD (pg)	Sensitivity (counts pg^{-1})	LOD (μg L^{-1})	ALOD (pg)	Sensitivity (counts pg^{-1})
^{55}Mn	0.073	0.29	278 600 ± 5200	0.094	16	14 200 ± 180
^{59}Co	0.021	0.084	203 800 ± 3700	0.0020	0.34	10 710 ± 100
^{60}Ni	0.014	0.056	40 900 ± 660	0.035	6.0	2395 ± 31
^{65}Cu	0.029	0.116	45 400 ± 900	0.017	2.9	2479 ± 25
^{66}Zn	0.030	0.12	14 300 ± 290	0.012	2.0	1241 ± 13

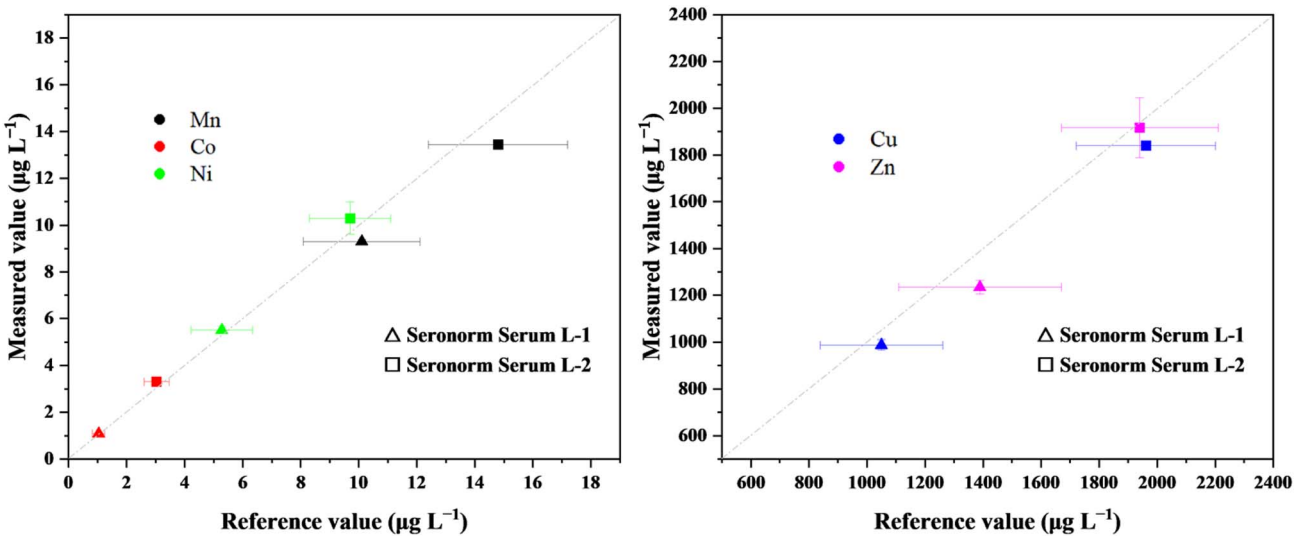

Fig. 5 Measurement results of elements in digested serum CRMs.

for measurement. As shown in Fig. 5 and Table S2, the measured values agreed well with the certified values, confirming that the established MUSDN-ICP-QMS method can accurately determine trace elements in minute biological samples with a very low sample consumption of only 4 μL per analysis.

Building upon the accuracy verified for digested samples, direct analysis without digestion was further attempted. Serum samples were simply diluted two-fold and analyzed under the same conditions. To evaluate the stability and reliability of the method during continuous operation, a 3-hour measurement sequence was conducted on 12 patient serum samples (each analyzed twice).

As summarized in Table 4, the concentrations of all five elements (Mn, Co, Ni, Cu, Zn) in L-2 were in good agreement with the certified reference values. Recoveries for L-2 ranged from 90.0% to 108%, all falling within 90–110%. The RSDs for L-2 ranged from 2.1% to 7.6%, indicating acceptable precision over the 3-hour period. Importantly, no systematic upward or downward trend was observed across the quality control measurements, and no clogging of the nebulizer occurred during the entire run, confirming that sample introduction issues were negligible. These results demonstrate that the proposed method, even without sample digestion, offers satisfactory stability and reproducibility for routine analysis of trace elements in undiluted or minimally diluted serum samples from clinical cohorts.

Table 4 Performance of Seronorm™ trace-element serum L-2 performance during 3-hour continuous analysis of 2-fold diluted, undigested serum samples (n = 4)

Parameter	Mn	Co	Ni	Cu	Zn
Reference value (μg L^{-1})	14.8 ± 2.4	3.03 ± 0.43	9.7 ± 1.4	1961 ± 239	1940 ± 270
Measured value (μg L^{-1})	13.3 ± 0.8	3.03 ± 0.23	9.56 ± 0.62	1770 ± 112	2100 ± 72
RSD (%)	2.1	7.6	6.5	6.4	3.4
Recovery (%)	90.0	99.9	98.6	90.3	108

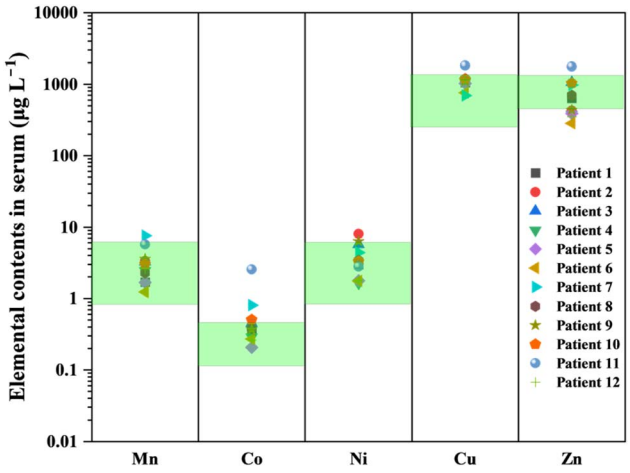

Fig. 6 Analytical results for undigested, 2-fold diluted serum samples from patients with colorectal cancer. The reference range of health individuals is indicated in green.

Fig. 6 presents the measured concentrations of Mn, Co, Ni, Cu, and Zn in undigested, two-fold diluted serum samples from 12 patients with colorectal cancer, alongside the reference ranges for healthy individuals.[34,35] The distribution patterns relative to the reference ranges varied among elements: Mn concentrations were evenly distributed within the reference interval across patients; Co levels were mostly located in the upper half of the reference range, with three cases exceeding the range; Ni concentrations were also predominantly in the upper half of the interval; Cu levels were similarly concentrated in the upper portion of the reference range; while Zn concentrations showed a relatively even distribution, with the overall range extending slightly beyond both ends of the reference interval. The method we have developed provides a new approach for the rapid and sensitive analysis of serum elements.

Conclusion

In this work, a MUSDN sample introduction system coupled with ICP-QMS was successfully developed for the highly sensitive, multi-element determination of transition metals in micro-volume biological samples. The method enables efficient and reliable analysis of trace metals in microliter-level serum samples, addressing a critical challenge in elemental bioanalysis. Systematic optimization demonstrated that the use of a platinum nebulizer sheet significantly reduced BECs, while a 4 μL droplet volume and Ge as an internal standard provided optimal analytical precision and stability. Compared to conventional PN-ICP-QMS, the MUSDN-ICP-QMS system demonstrated superior analytical sensitivity and significantly lower absolute detection limits, rendering it particularly advantageous for applications involving extremely limited sample volumes. Importantly, MUSDN exhibited excellent tolerance toward both high-salt and organic matrices. Matrix-induced signal suppression or enhancement from major serum components (*e.g.*, Na, Mg, Ca, and K) could be effectively compensated through Ge internal standardization, enabling accurate quantification even under complex matrix conditions. This robustness suggests that the method is compatible with simplified sample preparation strategies, such as direct dilution of serum samples, without compromising analytical accuracy. The successful determination of transition metals in certified serum reference materials further confirmed the method's accuracy, precision and practical applicability. Overall, the MUSDN-ICP-QMS provides a powerful tool for ultrasensitive multi-element analysis in micro-volume samples, with significant potential for applications in clinical diagnostics, biological research and environmental monitoring.

Author contributions

Yang Yu: writing – original draft, writing – review & editing, conceptualization, investigation, data curation; Junhang Dong: conceptualization, methodology, writing – original draft, data curation; Baoliang Zhong: resources, supervision; Xiaoqing Jin: resources, supervision; Zhujun Dai: investigation, data curation; Linjie Chen: writing – review & editing, conceptualization; Yu Li: data curation; Jing Chen: resources, supervision; Huan Tian: resources, supervision; Hongtao Zheng: methodology, supervision; Xing Liu: supervision, conceptualization; Zhenli Zhu: conceptualization, supervision, methodology, resources, project administration, writing – review & editing, funding acquisition.

Conflicts of interest

There are no conflicts to declare.

Data availability

Research data has been supplied *via* a repository doi: https://doi.org/10.17632/gfx9mwwy2t.2.

Supplementary information (SI) is available. See DOI: https://doi.org/10.1039/d6ja00052e.

Acknowledgements

This work was supported by the Natural Science Foundation of Hubei Province (2025AFA048), Hubei Provincial Health and Family Planning Commission General Project (WJ2023M141) and National Natural Science Foundation of China (22274145).

References

1 J. E. Johnson, T. M. Present and J. S. Valentine, *Proc. Natl. Acad. Sci. U. S. A.*, 2024, **121**, e2318692121.
2 A. Fontes, A. T. Jauch, J. Sailer, J. Engler, A. M. Azul and H. Zischka, *Int. J. Mol. Sci.*, 2024, **25**, 7880.
3 L. M. Li and X. B. Yang, *Oxid. Med. Cell. Longevity*, 2018, **2018**, 7580707.
4 G. Genchi, G. Lauria, A. Catalano, A. Carocci and M. S. Sinicropi, *Biology*, 2023, **12**, 1335.
5 J. C. Fontecilla-Camps, *Metallomics*, 2022, **14**, mfac016.

6 S. Blockhuys, E. Celauro, C. Hildesjö, A. Feizi, O. Stål, J. C. Fierro-González and P. Wittung-Stafshede, *Metallomics*, 2017, **9**, 112–123.
7 W. Maret, *Int. J. Mol. Sci.*, 2017, **18**, 2285.
8 B. N. Chen, P. Y. Yu, W. N. Chan, F. D. Xie, Y. G. Zhang, L. Liang, K. T. Leung, K. W. Lo, J. Yu, G. M. K. Tse, W. Kang and K. F. To, *Signal Transduction Targeted Ther.*, 2024, **9**, 6.
9 W. Y. Wang, W. T. Mo, Z. S. Hang, Y. Y. Huang, H. Yi, Z. J. Sun and A. W. Lei, *ACS Nano*, 2023, **17**, 19581–19599.
10 W. C. Wang, X. Liu, C. W. Zhang, F. Sheng, S. J. Song, P. H. Li, S. Q. Dai, B. Wang, D. W. Lu, L. Y. Zhang, X. Z. Yang, Z. H. Zhang, S. J. Liu, A. Q. Zhang, Q. Liu and G. B. Jiang, *Chem. Sci.*, 2022, **13**, 1648–1656.
11 P. Tsvetkov, S. Coy, B. Petrova, M. Dreishpoon, A. Verma, M. Abdusamad, J. Rossen, L. Joesch-Cohen, R. Humeidi, R. D. Spangler, J. K. Eaton, E. Frenkel, M. Kocak, S. M. Corsello, S. Lutsenko, N. Kanarek, S. Santagata and T. R. Golub, *Science*, 2022, **375**, 1254–1261.
12 B. Gardner, B. V. Dieriks, S. Cameron, L. H. S. Mendis, C. Turner, R. L. M. Faull and M. A. Curtis, *Sci. Rep.*, 2017, **7**, 10454.
13 I. V. Popescu, C. Stihi, G. V. Cimpoca, G. Dima, G. Vlaicu, A. Gheboianu, I. Bancuta, V. Ghisa and G. State, *Rom. J. Phys.*, 2009, **54**, 741–746.
14 R. Guo, H. M. Yu, S. B. Fang, Z. C. Xiao and F. Huang, *J. Anal. At. Spectrom.*, 2023, **38**, 2365–2377.
15 M. Aranaz, E. Valencia-Agudo, L. Lobo and R. Pereiro, *J. Anal. At. Spectrom.*, 2022, **37**, 50–68.
16 Z. H. Lv, J. X. Liu, X. F. Mao, X. Na and Y. Z. Qian, *Anal. Chim. Acta*, 2022, **1231**, 340444.
17 R. Brown, D. J. Gray and D. Tye, *Water, Air, Soil Pollut.*, 1995, **80**, 1237–1245.
18 J. H. Dong, C. Yang, D. He, H. T. Zheng, S. H. Hu and Z. L. Zhu, *At. Spectrosc.*, 2020, **41**, 57–63.
19 J. H. Dong, C. Yang, H. Q. Ding, P. J. Xing, F. Y. Zhou, H. Tian, X. Liu, H. T. Zheng, S. H. Hu and Z. L. Zhu, *Anal. Chem.*, 2021, **93**, 13351–13359.
20 D. He, Z. L. Zhu, X. Miao, H. T. Zheng, X. L. Li, N. S. Belshaw and S. H. Hu, *Microchem. J.*, 2019, **148**, 561–567.
21 S. Alavi, X. M. Guo, S. M. Javid, A. Ebrahimi and J. Mostaghimi, *Anal. Chem.*, 2020, **92**, 11786–11794.
22 P. Louvat, M. Tharaud, M. Buisson, C. Rollion-Bard and M. F. Benedetti, *J. Anal. At. Spectrom.*, 2019, **34**, 1553–1563.
23 H. T. Chen, S. Q. Cao and X. J. Zeng, *Chin. J. Anal. Chem.*, 2001, **29**, 592–600.
24 Y. Takasaki, K. Inagaki, A. Sabarudin, S. I. Fujii, D. Iwahata, A. Takatsu, K. Chiba and T. Umemura, *Talanta*, 2011, **87**, 24–29.
25 M. G. Minnich, D. C. Miller and P. J. Parsons, *Spectrochim. Acta, Part B*, 2008, **63**, 389–395.
26 J. W. Olesik, J. A. Hartshorne, N. Casey, E. Linard and J. R. Dettman, *Spectrochim. Acta, Part B*, 2021, **176**, 106038.
27 F. X. Du, X. G. Ma, F. Yuan, C. Wang, D. Snizhko, Y. R. Guan and G. B. Xu, *Anal. Chem.*, 2020, **92**, 4755–4759.
28 C. D. Meng, F. X. Du, A. Abdussalam, A. M. Wang, D. Snizhko, W. Zhang and G. B. Xu, *Anal. Chem.*, 2021, **93**, 14934–14939.
29 Y. Y. Li, J. Tang, Y. H. Xiao, T. Ren, J. H. Yang, Y. Lin and C. B. Zheng, *Anal. Chem.*, 2024, **96**, 7187–7193.
30 J. H. Dong, J. Z. Liu, P. J. Xing, S. Y. Li, J. S. Piao, H. F. Tao, L. J. Li, H. T. Zheng, Z. Zhang, S. R. Han, X. Liu and Z. L. Zhu, *Anal. Chem.*, 2023, **95**, 6271–6278.
31 J. H. Dong, Y. Yu, Z. J. Dai, S. Y. Li, L. J. Chen, P. J. Xing, G. Wang, X. Liu, H. T. Zheng and Z. L. Zhu, *Anal. Chem.*, 2024, **96**, 19955–19964.
32 C. Agatemor and D. Beauchemin, *Anal. Chim. Acta*, 2011, **706**, 66–83.
33 G. Grindlay, J. Mora, M. de Loos-Vollebregt and F. Vanhaecke, *Spectrochim. Acta, Part B*, 2013, **86**, 42–49.
34 N. Laur, R. Kinscherf, K. Pomytkin, L. Kaiser, O. Knes and H. P. Deigner, *PLoS One*, 2020, **15**, e0233357.
35 J. M. Harrington, D. J. Young, A. S. Essader, S. J. Sumner and K. E. Levine, *Biol. Trace Elem. Res.*, 2014, **160**, 132–142.